Journal of Ovonic Research Vol. 14, No. 1, January - February 2018, p. 63 - 69

FABRICATION AND CHARACTERIZATION OF ZnO@ZnS CORE-SHELL STRUCTURES ON ITO SUBSTRATES

W. C. HUANG[a], Y. T. CHEN[b], W. C. WENG[b], J. L. CHIU[b], C. Y. LI[b], Y. S. TSAI[b], P. C. LIN[b], C. C. LU[b], W. M. SU[b], C. F. LIN[c], Y. S. LIN[d], H. CHEN[b*]

[a]*Department of Electro-Optical Engineering,, Kun Shan University, Taiwan, ROC*
[b]*Department of Applied Material and Optoelectronic Engineering, National ChiNan University, Taiwan, ROC*
[c]*Department of Materials Science and Engineering, National Chung Hsing University, Taiwan, ROC*
[d]*Department of Chemical Engineering, Feng Chia University, Taiwan, ROC*

In this research, ZnO@ZnS core-shell structures are fabricated on ITO substrates. To characterize the ZnO@ZnS nanostructures, multiple material and optical characterizations are performed. Results indicate that fluffy ZnS shell can be grown on ZnO nanorods. Moreover, the defect luminescence can be suppressed by coating ZnS shell on the ZnO nanostructures. ITO/ZnO@ZnS structures are promising for future optoelectronic device applications.

(Received November 23, 2017; Accepted February 6, 2018)

Keywords: ZnS, ITO, core-shell structures, oxygen vacancy, fluffy

1. Introduction

Owing to chemical stability, wide-bandgap and high exciton binding energy, 1D ZnO nanostructures [1] have been widely utilized in optoelectronic applications. However, high defect concentration in ZnO related materials [2] may cloud the development of ZnO electrical and optical devices. To enhance ZnO-based optoelectronic material performance [3,4,5] and suppress defect luminescence, ZnO@ZnS core-shell structures [6,7] are proposed as hetero-nanostructures [8,9] to boost electro-optical conversion efficiency [10,11,12,13]. ZnO@ZnS core-shell nanostructures are formed by coating ZnS on the surface of ZnO nanorods [14,15]. It can be seen that the solgel/hydrothermal growth of ZnO NRs and ZnO@ZnS core-shell NRs are shown in Fig. 1(a) and (b), respectively. ZnS has a bandgap of 3.6 eV [16,17,18], which is larger than ZnO of 3.37 eV. ZnO@ZnS cores-shell can be formed by anion exchange on ZnO nanorods during hydrothermal growth [19,20]. In this study, we fabricate ZnO@ZnS nanostructures on indium tin oxide (ITO). To characterize the core-shell, scanning electron microscope (SEM), energy dispersive X-ray spectroscopy (EDX), contact angle analyze, X-ray diffraction (XRD), photoluminescence (PL), Raman analysis and X-ray photoelectron spectroscopy (XPS) are performed on the nanostructures. Results indicate that ZnS can be appropriately coated on ZnO NRs with growth time of 20 min. Furthermore, sulfur content and ZnS crystalline phases can be confirmed by EDX and XRD. Furthermore, defect luminescence suppression can be observed by PL and XPS measurements. ITO/ZnO@ZnS structures show promises for future optoelectronic device applications [21, 22, 23, 24].

*Corresponding author: hchen@ncnu.edu.tw

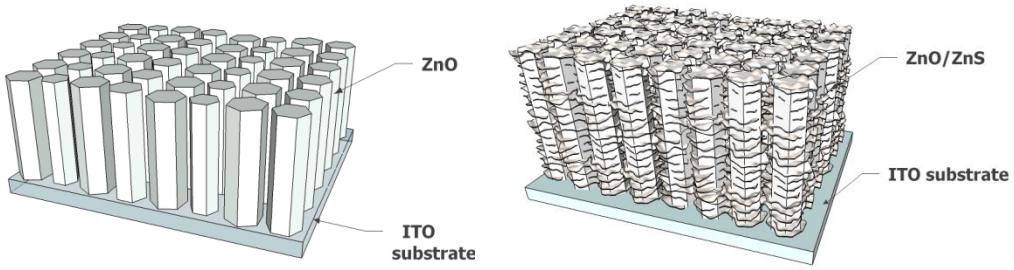

(a) (b)

Fig. 1 Illustrations of (a) ZnO NRs (b) ZnO/ZnS core-shell NRs structures.

2. Experimental

ITO transparent conductive substrates are cut into 2 cm * 2 cm size. Then, the substrates were cleansed with ethanol, acetone, and isopropyl alcohol for 10 mins. To obtain uniform and high-quality ZnO NRs, ZnO seed layers were spread by sol-gel methods. The sol-gel solution contains $Zn(CH_3COO)_2$ 0.05 M and several drops of monoethanolamine (MEA). After the seed layer is spin coated on the substrate, ZnO NRs are grown by hydrothermal methods with 100 ml solution containing $Zn(NO_3)_2$ 0.05 M and 0.07 M hexamethylenetetramine (HMTA). In this process, HMTA stably releases OH^- and forms a complex with Zn^{2+}, and then the complex dehydrates to precipitate the ZnO crystal. In order to minimize the free energy in the system, ZnO will grow along the non-polar plane, and promote the anisotropy growth in the c-axis direction to form a one-dimensional nanocolumn structure on the ITO substrate. The temperature of the solution is kept at 80 ^oC for the growth time of 1 hour. After ZnO NRs are grown on the substrates, ZnS shell is deposited on the ZnO NRs by a second-step hydrothermal growth. The second-step hydrothermal solution contains 0.1 M $Na_2S \cdot 9\ H_2O$ 100 ml. ZnS shell structures are grown at a temperature of 60 ^oC for the growth time of 20 and 30 mins. ZnO@ZnS core-shell structures can be obtained by anion exchange during hydrothermal growth.

3. Results and discussion

To reveal the surface morphologies of ZnO and ZnO@ZnS, FESEM is used to view the microstructures. Fig.2 (a) shows that high-quality ZnO nanorods are grown along the c-axis on a ITO substrate and the diameter of ZnO NRs are 30 to 40 nm. After the ZnS shell is grown for 20 mins, ZnS nanopowder is spread on the surface of ZnO NRs as shown in Fig.2 (b) and the the rod diameters on the ITO/ZnO@ZnS structure increased to 40 to 60 nm. Fig. 2 (c) shows the ZnS is further grown for 30 mins, the fluffy-like ZnS nanostructure can be observed along the side surface of the ZnO NRs and the rod diameter of the NRs of the ITO/ZnO@ZnS structure was further increased to 60 to 70 nm. Consistent with the FESEM images, EDX analysis for the ZnO@ZnS structure with the growth time of 20 mins as shown in Fig.3 (b) reveals that the content of sulfur is around 5.19 %. As the growth time of ZnS increases, the content of sulfur is increased to 9.55 % as shown in Fig.3 (c).

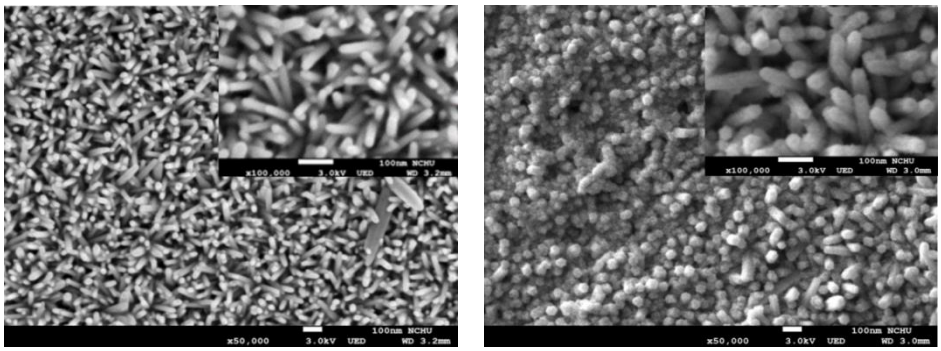

(a) (b)

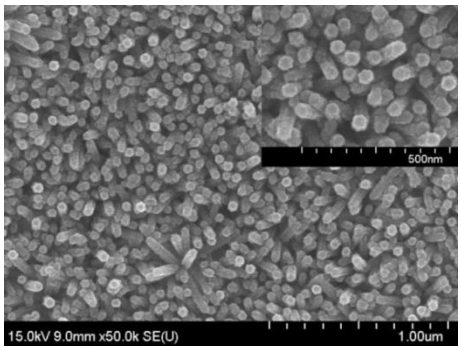

(c)

Fig. 2 FESEM images of the ZnO/ZnS core-shell nanostructures with deposition time of (a) 0 min (b) 20 min (c) 30min.

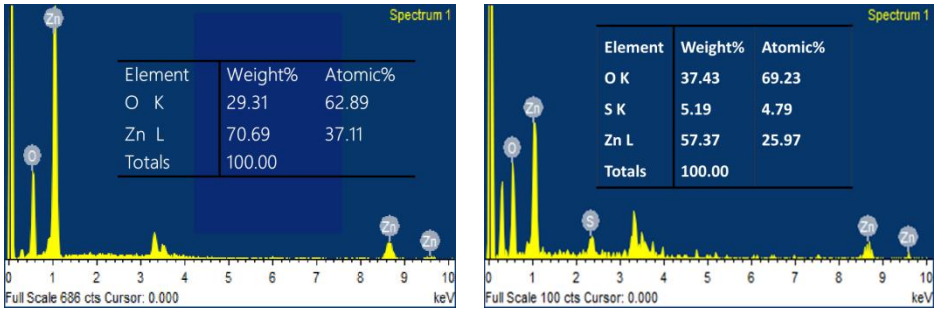

(a) (b)

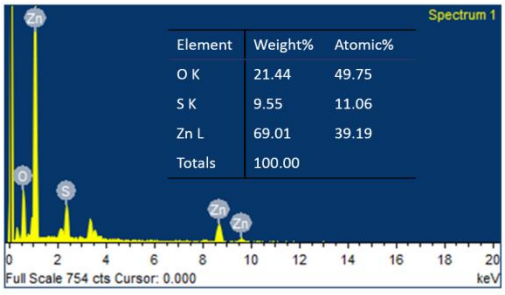

(c)

Fig. 3 EDX analysis for the ZnO/ZnS structures with the ZnS growth time of (a) 0 min (b) 20 min (c) 30min

On the other hand, to study hydrophobicity of the nanostructures, Fig.4 (a), (b), and (c) show the contact angle measurements. Results show that ZnS can cause the surface to have hydrophilicity and cause the contact angle smaller. Furthermore, since ZnS layer with growth time of 20 mins as shown in Fig.4 (b) may spread near the surface, ZnO@ZnS nanostructures with growth time of 20 mins has the least surface contact angle.

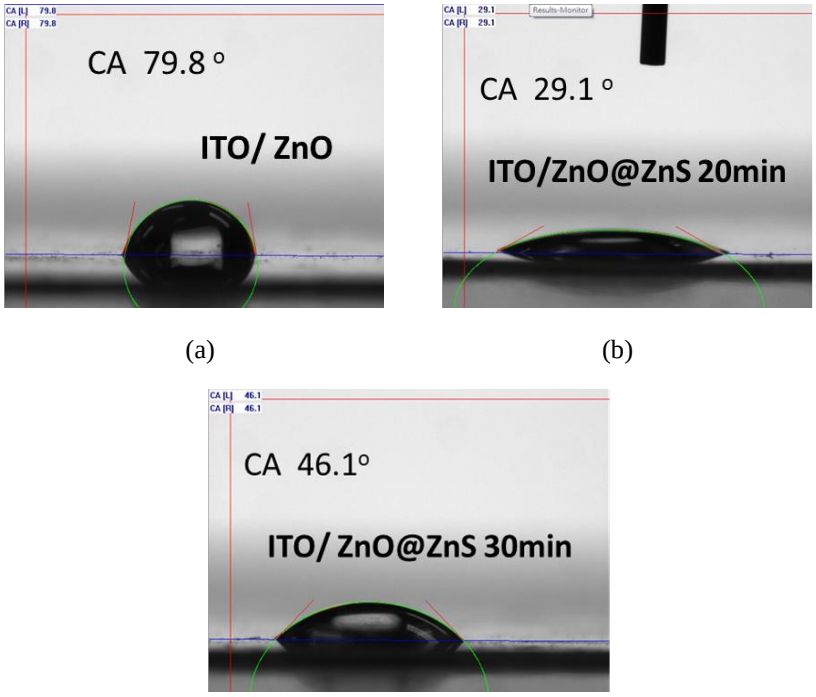

Fig. 4. Surface contact angle measurements of the ZnO/ZnS nanostructures with ZnS deposition time of (a) 0 (b) 20 (c) 30 min.

Furthermore, to examine the crystalline structures of ZnO and ZnS, XRD is used to analyze the ZnO@ZnS core-shell structures. Fig.5 shows the crystalline phases of ZnO, ZnO@ZnS nanostructures with the growth time of 20 mins and 30 mins. Results indicate that ZnS (220) appear after the ZnS is coated on ZnO NRs. Furthermore, ZnS (220) are enhanced as the growth time increased to 30 mins which represents the stable growth of ZnS shell.

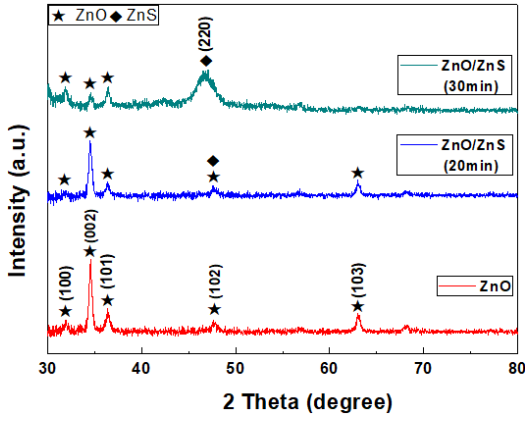

Fig. 5. XRD patterns of the ZnO/ZnS structures with the ZnS deposition time of 20 and 30 mins

Moreover, to study the optical properties of ZnO and ZnO/ZnS structures, PL is used to examine the near band-edge (NBE) emission with PL peak around 395 nm, and oxygen- related defect luminescence with PL peak around 560 nm. As shown in Fig.6, results indicate that NBE/defect luminescence ratio can be strengthened after ZnS is coated. Furthermore, as the ZnS is grown for 20 mins, defect luminescence can be greatly suppressed. Since ZnS can compensate oxygen related defects as previous studies indicated, defect luminescence can be greatly diminished. In addition, the NBE peak slightly blue-shift from 392 nm to 388 nm after ZnS is deposited on ZnO NRs.

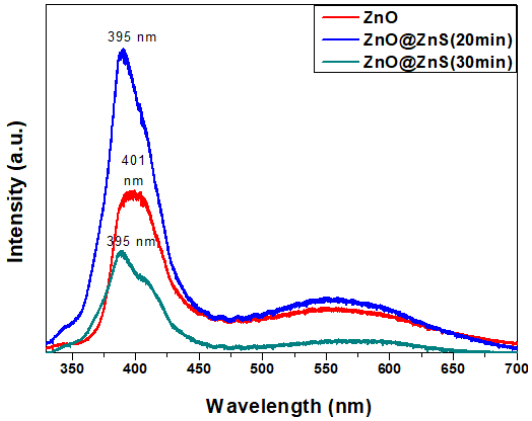

Fig. 6. PL measurements of the ZnO/ZnS structures with different ZnS deposition time

Moreover, Raman analysis reveals that ZnO peak around 578 cm^{-1} is present for the ZnO NRs as shown in Fig.7. Furthermore, after ZnS is coated on the ZnO NRs, ZnS-like LO, peak around 345 cm^{-1} emerges [25]. Moreover, ZnS-like LO, peak is enhanced as the ZnS growth time increases from 20 mins to 30 mins.

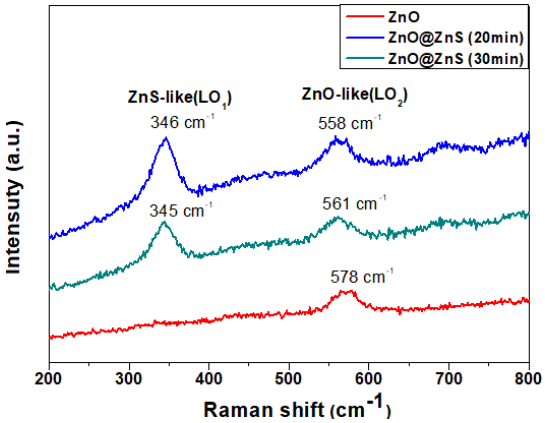

Fig. 7. Raman measurements of the ZnO/ZnS structures with different ZnS deposition time

Comparison of XPS spectra of NRs before and after sulfuration process is shown in Fig. 8, the S 2p peak and S 2s emerged as the ZnS structures grown on ZnO NRs in contrast to the pure ZnO NRs, while all the other O and Zn spectra were similar.

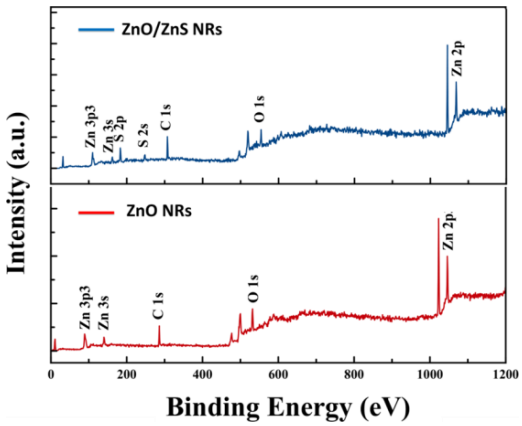

Fig. 8 The XPS spectra of ZnO NRs and ZnO/ZnS core-shell NRs

4. Conclusions

In this study, ZnS is successfully synthesized on the ZnO NRs to form ZnO@ZnS core-shell structures on ITO substrates. Multiple material and optical analysis indicate that the appropriate coating of ZnS can enhance ZnS crystalline structures and suppress defect luminescence. The ITO/ZnO@ZnS nanostructures show promises for future optoelectronic device applications.

References

[1] V. Kumar, N. Singh, R. Mehra, A. Kapoor, L. Purohit and H. Swart, Thin Solid Films **539**, 161 (2013).
[2] Y. Hou and A. H. Jayatissa, Thin Solid Films **562**, 585 (2014).
[3] K. Ranjith, P. Saravanan, V. Vinod, J. Filip, M. Černík, R. R. Kumar, Catalysis Today **278**, 271 (2016).
[4] M.-H. Hsu, C.-J. Chang, H.-T. Weng, ACS Sustainable Chemistry & Engineering **4** (3), 1381 (2016).
[5] L. Yang, H. Luan, G. Chen, Y. Sun, X. Kong, J. Yang, Journal of Materials Science: Materials in Electronics **26** (9), 6986 (2015).
[6] H. Haddad, A. Chelouche, D. Talantikite, H. Merzouk, F. Boudjouan and D. Djouadi, Thin Solid Films **589**, 451 (2015).
[7] A. Kushwaha and M. Aslam, Electrochimica Acta **130**, 222 (2014).
[8] J. Xu, H. Sang, X. Wang and K. Wang, Dalton Transactions **44** (20), 9528 (2015).
[9] H. Kermani, H. R. Fallah, M. Hajimahmoodzadeh and N. Basri, Thin Solid Films **539**, 222 (2013).
[10] H. Li, S. Jiao, H. Li, S. Gao, J. Wang, D. Wang, Q. Yu, Y. Zhang, L. Li and H. Zhou, RSC Advances **6** (78), 74575 (2016).
[11] A. Brayek, S. Chaguetmi, M. Ghoul, I. B. Assaker, A. Souissi, L. Mouton, P. Beaunier, S. Nowak, F. Mammeri and R. Chtourou, RSC Advances **6** (37), 30919 (2016).
[12] M. Wang, H. Qin, Y. Fang, J. Liu and L. Meng, RSC Advances **5** (127), 105324 (2015).
[13] M. Sookhakian, Y. Amin, S. Baradaran, M. Tajabadi, A. M. Golsheikh and W. Basirun, Thin Solid Films **552**, 204 (2014).
[14] W. Riedel, Y. Fu, Ü. Aksünger, J. Kavalakkatt, C.-H. Fischer, M. C. Lux-Steiner, S. Gledhill, Thin Solid Films **589**, 327 (2015).
[15] D. Bao, P. Gao, X. Zhu, S. Sun, Y. Wang, X. Li, Y. Chen, H. Zhou, Y. Wang and P. Yang,

Chemistry-A European Journal **21** (36), 12728 (2015).
[16] M. T. Man and H. S. Lee, Current Applied Physics **15** (7), 761 (2015).
[17] S. Ummartyotin and Y. Infahsaeng, Renewable and Sustainable Energy Reviews **55**, 17 (2016).
[18] H. Hennayaka and H. S. Lee, Thin Solid Films **548**, 86 (2013).
[19] D. Guo, K. Sato, S. Hibino, T. Takeuchi, H. Bessho and K. Kato, Thin Solid Films **550**, 250 (2014).
[20] M. Mehrabian, H. Afarideh, K. Mirabbaszadeh, L. Lianshan and T. Zhiyong, Journal of the Optical Society of Korea **18** (4), 307 (2014).
[21] H. Lin, L. Wei, C. Wu, Y. Chen, S. Yan, L. Mei and J. Jiao, Nanoscale research letters **11**(1), 420 (2016).
[22] H. Yan, T. Li, Y. Lu, J. Cheng, T. Peng, J. Xu, L. Yang, X. Hua, Y. Liu and Y. Luo, Dalton Transactions **45** (44), 17980 (2016).
[23] A. K. Giri, C. Charan, S. C. Ghosh, V. K. Shahi and A. B. Panda, Sensors and Actuators B: Chemical **229**, 14 (2016).
[24] S. Zhang, B. Yin, H. Jiang, F. Qu, A. Umar and X. Wu, Dalton Transactions **44** (5), 2409 (2015).
[25] X. Shuai and W. Shen, The Journal of Physical Chemistry C **115** (14), 6415 (2011).